

Species Delineation Within the *Euwallacea fornicatus* (Coleoptera: Curculionidae) Complex Revealed by Morphometric and Phylogenetic Analyses

Demian F. Gomez,¹ James Skelton,¹ M. Sedonia Steininger,² Richard Stouthamer,³ Paul Rugman-Jones,³ Wisut Sittichaya,⁴ Robert J. Rabaglia,⁵ and Jiri Hulcr^{1,6,7}

¹School of Forest Resources and Conservation, University of Florida, 136 Newins-Ziegler Hall, Gainesville, FL 32611, ²Agricultural Research Service, USDA, 1600-1700 SW 23RD DRIVE, Gainesville, FL 32608, ³Department of Entomology, University of California, 3401 Watkins Drive, Riverside, CA 92521, ⁴Department of Entomology, Prince of Songkla University, 15 Karnjanavanich Road, Hat Yai, Songkhla 90110, Thailand, ⁵Forest Health Protection, USDA-Forest Service, 201 14 Street, SW, Washington, DC 20250, ⁶Entomology and Nematology Department, University of Florida, 1881 Natural Area Drive, Gainesville, FL 32611, and ⁷Corresponding author, e-mail: hulcr@ufl.edu

Subject Editor: Bjarte Jordal

Received 24 May 2018; Editorial decision 22 October 2018

Abstract

The ambrosia beetle *Euwallacea fornicatus* Eichhoff sensu lato is a complex of genetically divergent emerging pests responsible for damages to tree industries and ecosystems around the world. All lineages within the species complex are currently considered morphologically identical, presenting problems for their delineation and highlighting the shortcomings of species concepts based solely on type-specimen morphology. The objectives of this work were to 1) broaden the geographic sampling of the *E. fornicatus* complex in Asia, 2) reconstruct relationships between clades and populations, 3) find morphological characters or combinations of characters which are useful in delimiting the genetic lineages of the *E. fornicatus* species complex, and 4) propose taxonomic delimitation of species where morphology and phylogenetic identity correlate. Our integrated approach using molecular and morphological evidence suggests four clades that differ morphologically, but with overlap, therefore, cytochrome oxidase c subunit I (COI) barcoding remains necessary for assigning specimens to a clade. The following taxonomic changes are proposed: *E. fornicatus* (Eichhoff 1868) (= 'Tea Shot Hole Borer Clade a'); *E. fornicator* (Eggers 1923), stat. rev. (= 'Tea Shot Hole Borer Clade b'); *E. whitfordiodendrus* (Schedl 1942), stat. rev. (= 'Polyphagous Shot Hole Borer'); and *E. kuroshio* Gomez and Hulcr, sp. nov. (= 'Kuroshio Shot Hole Borer'). This approach delivers a practical, evidence-based guidance for species delineation that can address overlapping variation in morphological characters of an emerging pest species complex.

Key words: Ambrosia beetle, cryptic species, invasive species, morphology

Species identity is foundational to all of biology. It becomes particularly important in organisms whose biology defies the assumptions of the standard species concepts, such as where barriers between biological species are porous, or in clonal organisms where variation does not transcend clones. The need to correctly delimit species is becoming increasingly important also for applied biology and biosecurity research (Hurley et al. 2017). Unusual reproductive strategies are overrepresented among invasive species, as clonal, inbred and otherwise unusually reproducing organisms are often more successful at colonizing new regions than regularly sexually reproducing ones (Brockerhoff and Liebhold 2017), particularly when considering the many forest pests and pathogens that are morphologically cryptic.

Some of the most morphologically cryptic, economically damaging, and frequently intercepted pests are ambrosia beetles in the tribe Xyleborini (Coleoptera: Curculionidae: Scolytinae) (Haack 2001). Of the 60 nonnative scolytines established in the United States (Haack and Rabaglia 2013), 30 are xyleborines (Atkinson 2017). The haplodiploid mating system within this tribe, their small size (many species are <2 mm in length), their wood-boring habit, and their relationships with ambrosia fungi, make the ambrosia beetles highly successful invaders (Jordal et al. 2001). One of the most cost-effective options for the prevention of invasive scolytine establishment is the enforcement of phytosanitary standards (Susaeta et al. 2016). However, a key issue in this approach is the ability to correctly identify the incoming invaders (Armstrong and Ball 2005).

One exceptionally successful invader is the xyleborine species *Euwallacea fornicatus* Eichhoff 1868 (Curculionidae: Scolytinae), commonly called the Tea Shot Hole Borer (TSHB). This species impacts tea (*Camelia sinensis*) in at least 10 different countries (Li et al. 2015), including India and Sri Lanka where it is a major economic pest (Danthanarayana 1968). Beetles matching the species description for *E. fornicatus* were recently introduced into Israel, where they inflict severe damage to several tree species (Mendel et al. 2012). Specimens from Israel were later found to be genetically different from Sri Lankan beetles (O'Donnell et al. 2015, Stouthamer et al. 2017). Specimens of *E. fornicatus* with the same genetic identity as those from Israel were later confirmed as causing damage to trees in California (United States) in 2012, where it was first recorded in 2003 (Eskalen et al. 2012). Specimens of *E. fornicatus* which were genetically closer to Sri Lankan beetles were also initially documented in Florida in 2002 with minor impacts on a few hosts (Rabaglia et al. 2006), and later on avocados in 2012, with increasing levels of damage since then (Carrillo et al. 2016). In addition to the genetic divergence of *E. fornicatus* beetles in Israel and California from those in Florida and Sri Lanka, it was also reported that the fungal symbionts of the respective populations were also morphologically and genetically distinct. Indeed, beetles from the Israel and California populations could not survive on the fungi of the pestiferous beetle species on tea (Freeman et al. 2012). However, the extent of such beetle-fungus specificity is challenged by several studies showing that species of *Euwallacea* Hopkins, 1915 (Curculionidae: Scolytinae) switch or share symbionts (Kasson et al. 2013, O'Donnell et al. 2015, Dodge et al. 2017).

The increasing damage caused by the *E. fornicatus* complex to tree industries and ecosystems in the United States and abroad is of great importance to scientists, regulators and tree health practitioners (García-Avila et al. 2016). Individual populations, some of which appear to cause greater damage than others, are currently considered morphologically indistinguishable (Chen et al. 2016). The confusion is compounded by the fact that the type specimen of *E. fornicatus*, which was collected from Sri Lanka, was destroyed in World War II, and the only remaining information about it is from the brief, original description (Eichhoff 1868). Subsequently, five species have been synonymized with *E. fornicatus* (*Xyleborus fornicatior* Eggers 1923, *X. whitfordiodendrus* Schedl 1942, *X. perbrevis* Schedl 1951, *X. schultzei* Schedl 1951, and *X. tapatapaoensis* Schedl 1951) (Curculionidae: Scolytinae) (Wood 1989, Beaver 1991, Beeson 1930). Descriptions of species that were separated from *E. fornicatus* are also brief, and typically follow the typological species concept where intraspecific variability is not examined. Ambiguous species descriptions, lack of type material, and overlapping morphological variability within this group have resulted in confusion about the true identity of economically and environmentally damaging *E. fornicatus* populations.

A recent phylogenetic assessment of *E. fornicatus* in the United States and elsewhere identified three major genetic lineages (clades) within the *E. fornicatus* species complex (Stouthamer et al. 2017). The lineages generally correlated with phylogeographic patterns in both native and invaded regions. The lineage designated *E. fornicatus* sensu stricto (commonly called the TSHB), is originally from southern Southeast Asia and was introduced into the U.S. states of Hawaii and Florida. A second lineage (called the Kuroshio Shot Hole Borer or KSHB) probably originated in Taiwan and Japan, and was introduced into San Diego County in California (United States) and Mexico (García-Avila et al. 2016). The third lineage is likely from Southeast Asia and was introduced into Los Angeles County, California (United States), along with Israel, and South

Africa (Stouthamer et al. 2017, Paap et al. 2018). This last lineage has been given the common name Polyphagous Shot Hole Borer (PSHB) in reference to its very broad host range. PSHB is associated with several phytopathogenic *Fusarium* species and is causing significant damage to avocado production, urban and natural vegetation (Eskalen et al. 2012, Boland 2016). Despite differences in fungal symbionts, geographic range, and host preference among these genetic lineages of *E. fornicatus*, diagnostic morphological characters have not yet been described.

The objectives of this work were to 1) broaden the geographic sampling of the *E. fornicatus* complex in Asia, 2) reconstruct relationships between clades and populations, 3) find morphological characters or combinations of characters which are useful in delimiting the genetic lineages of the *E. fornicatus* cryptic species complex, and 4) propose taxonomic delimitation of species where morphology and phylogenetic identity correlate. We tested the hypothesis that there are quantifiable, diagnostic morphological differences between the three genetic lineages. Rather than using the traditional typological species concepts, we define putative species by the correlation between variation in multiple morphological features and phylogenetic placement, defined using multivariate analysis and regression-based classification. Identifying and quantifying morphological differences may allow for the creation of an identification tool for use by researchers and agencies. Additionally, using historical museum material, we tested whether the newly defined phenotypes fit any of the previously described species in or near the *E. fornicatus* complex to clarify their taxonomic identity.

Methods

Specimens

Eighty-nine specimens were measured and genotyped from 26 localities in 11 countries (China, Hong Kong, Indonesia, Japan, Papua New Guinea, American Samoa, Singapore, Taiwan, Thailand, United States, and Vietnam). These populations were selected as representing the known native and introduced distribution (Supp. Table S1).

DNA Extraction and Sequence Generation

Specimens were collected between 2009 and 2017 and deposited in the frozen collection in the Forest Entomology Lab managed by J.H. (University of Florida, Gainesville, FL). Additional specimens collected by R.S. in 2015 were used. Before the DNA extraction was conducted, specimens were surface-washed in a Tween solution via vortexing and EtOH rinse. DNA extractions were performed non-destructively with the DNEasy Blood and Tissue Kit (Qiagen, Carlsbad, CA) by puncturing 2 or 3 holes between the pronotum and the abdomen ventrally preserving the overall structure of the beetle, and then incubating the individuals for 3 h in Qiagen Proteinase K Lysis Buffer Solution. The specimens were then recovered and stored at -80°C . DNA was extracted from the remaining lysate using the Qiagen DNEasy protocol. The final product was eluted in 50 μl of the provided elution buffer. The mitochondrial gene cytochrome oxidase c subunit I (COI) was amplified through polymerase chain reaction (PCR) using the primer pair LCO1490 and HCO2198 (Folmer et al. 1994). PCR was conducted in 25 μl reactions. Two microliters of DNA were used as template. Positive and negative controls were performed. Thermocycling conditions were as follows: 96°C for 2 min followed by 40 cycles of denaturation at 94°C for 30 s, annealing at 57°C for 1 min and 30 s, and extensions at 72°C for 1 min, and a final extension 72°C for 5 min. Amplification was confirmed by electrophoresis on a 1% Agarose gel at 110 V for 45 min. PCR products were sent to Eurofins sequencing lab for sequencing in

Table 1. List of characters and character states examined

Character	Character states
Head	
Epistomal shape	Narrow, broad
Epistomal width	
Epistomal projection length	
Epistomal transverse impression	Slightly impressed, impressed
Frons shape	Direct comparison
Texture frons	Smooth, reticulated
Punctures frons	Sparse, abundant
Vestiture	Presence, absence
Vestiture abundance	Sparse, abundant
Location of vestiture	Direct comparison
Submentum shape	Direct comparison
Submentum size	Direct comparison
Eyes size	Upper part smaller than lower part, upper part similar than lower part
Insertion of antennae	Close to eyes, close to epistoma
Extent of emargination of eyes	Close to insertion of antennae, far from insertion of antennae
Eyes shape	Direct comparison
Antennae	
Scapus shape	Direct comparison
Scapus size	Short, large
Scapus setae	Presence, absence
Number of funicle segments	
Length of funicle relative to pedicel	Direct comparison
Pedicel shape	Direct comparison
Pedicel size	Short, large
Club shape	Direct comparison
Club length	Direct comparison
Shape of club sutures	Direct comparison
Segment 1 of club condition	Soft, corneous
Segment 2 of club condition	Soft, corneous
Segment 3 of club condition	Soft, corneous
Number of segments of club visible anteriorly	1, 2, 3
Number of segments of club visible posteriorly	1, 2, 3
Shape of sutures in club	Procurved, recurved
Pronotum	
Length	From base to apex in lateral view
Width	Measured in widest point
Overall shape in lateral view	Taller, rounded
Shape in dorsal view	Subquadrate, quadrate
Location of summit	Direct comparison
Asperities coverage	Sparse, abundant
Size of asperities	Small, medium, large
Arrangement of asperities	Direct comparison
Number of serrations on anterior margin	
Size of serrations on anterior margin	Small, medium, large
Punctures on lateral margin	
Punctures on lateral margin	Presence, absence
Location of punctures on lateral margin	Direct comparison
Size of punctures on lateral margin	Small, medium
Punctures on pronotal disc	
Punctures on pronotal disc	Presence, absence
Location of punctures on pronotal disc	Direct comparison
Abundance of punctures on pronotal disc	Direct comparison
Setae on lateral margin	Presence, absence
Location of setae	Direct comparison
Setae on dorsum	Presence, absence
Abundance of setae on dorsum	Sparse, medium, abundant
Shape of lateral costa	Direct comparison
Legs	
Procoxae condition	Contiguous, separated
Protibiae shape	Flattened, robust
Protibiae width	
Protibiae length	
Number of denticles in the protibiae	7,8,9,10,11
Position of denticles in the protibiae	Direct comparison

Table 1. Continued

Character	Character states
Size of denticle sockets in the protibiae	Direct comparison
Length of protibial bristle	
Width of protibial bristle	
Setae in protibiae	Sparse, abundant
Number of denticles in mesotibiae	
Shape of mesotibiae	Direct comparison
Number of denticles in metatibiae	
Shape of metatibiae	Direct comparison
Posterocoxae process length	
Posterocoxae process shape	Direct comparison
Elytra	
Length	From base to apex in lateral view
Width	At base
Overall shape in dorsal view	Direct comparison
Overall shape in lateral view	Direct comparison
Shape of elytra base	Direct comparison
Size of scutellum	Small, medium
Shape of scutellum	Direct comparison
Number of punctures on interstria 1–3	
Size of punctures on disc of interstria 1–3	Similar, different
Location of punctures	Direct comparison
Condition of punctures	Parallel, divergent
Number of interstriae	
Relative width of interstriae	
Condition of interstriae	Parallel, divergent
Overall shape of interstriae	Uniseriate, biseriate, confused
Number of striae	
Relative width of striae	
Condition of striae	Parallel, divergent
Overall shape of striae	Distinct, confused
Elytral declivity	
proportion of elytra	Direct comparison
shape in dorsal view	Direct comparison
shape in lateral view	Direct comparison
Shape of carina	Sharp, blunt
Size of carina	Medium, large
Location of carina	Direct comparison
Granules	Presence, absence
Location of granules	Direct comparison
Abundance of granules	Sparse, abundant
Interstrial vestiture	Sparse, medium, abundant
Location of setae	Direct comparison
Length of setae	Short, medium, long
Interstriae condition	Parallel, divergent
Size of punctures on interstria 1–3	Similar, different

Direct comparison refers to characters for which characters states were unknown, and which required direct comparison of specimens for the analysis of variability.

both forward and reverse directions. Forward and reverse sequences were trimmed (error probability less than 0.01) and checked for agreement using Geneious (Kearse et al. 2012). Sequences were aligned with MAFFT (Katoh and Standley 2013). Sequences were manually assessed for indels, frameshifts, or stop codons, suggesting low probability of NUMTs. No double peaks were observed in the most deviant sequences. Specimen consensus sequences were deposited on GenBank (accession numbers MH276907–MH276950).

Phylogenetic Reconstruction

Genealogical relationships among individual beetles were reconstructed using maximum likelihood (ML) analyses, conducted with RAxML (Stamatakis 2014) with the substitution model

GTRGAMMA and the ‘-f a’ fast bootstrapped tree method and 1,000 bootstrap replicates. Sequences of several other Xyleborini species were used to root the ML analysis. The resulting trees were graphically edited using Figtree (v1.4.3 - <http://tree.bio.ed.ac.uk/software/figtree>). Sequence divergence within and between clades was calculated as mean pairwise uncorrected p-distances and Kimura two-parameter distances (K2P) using Mega, version 7 (Kumar et al. 2016), as used in Stouthamer et al. (2017).

Morphological Analysis

One hundred two morphological characters were assessed in search of differences between clades in the *E. fornicatus* species complex (Table 1). Characters and measurements that show variation among

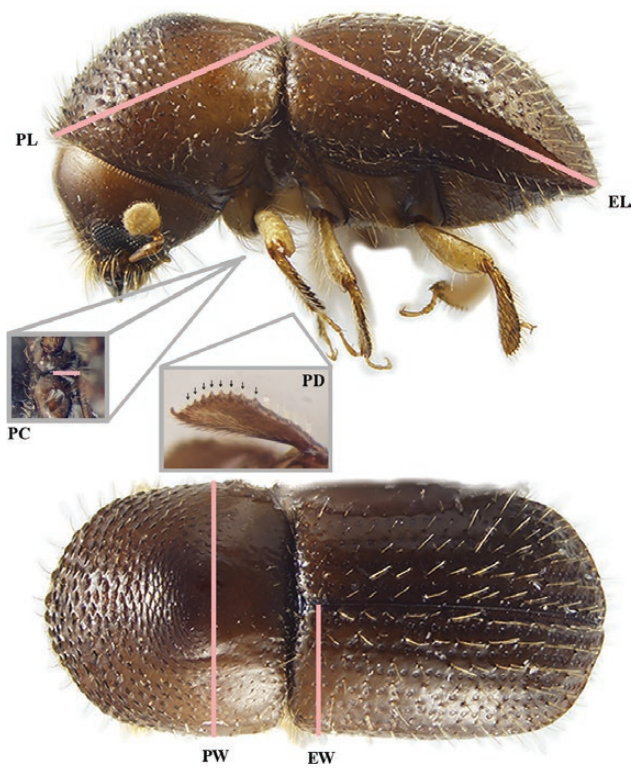


Fig. 1. Pink lines show relevant morphological characters in the *Euwallacea fornicatus* species complex: pronotum length (PL), pronotum width (PW), elytra length (EL), elytra width (EW), posterocoxal process length (PC), protibial socketed denticles (PD).

clades and were used in the statistical analysis are shown in Fig. 1. All characters were measured in females to the nearest 0.01 mm using a stereomicroscope Olympus SZX16 at 50 \times magnification. All statistical analyses were performed using R v.3.4.2 (R Development Core Team 2017), with the packages cluster (version 2.0.6), rpart (version 4.1–11), and vegan (version 2.4–4). Graphs and classification trees were generated with the packages graphics (version 3.4.2), ggplot2 (version 2.2.1), and rpart.plot (version 2.1.2).

Variation in morphology among clades was visualized by ordination using non-metric multidimensional scaling (NMDS, metaMDS {vegan}). To statistically test for differences between the clades, a permutational multivariate analysis of variance (PERMANOVA, Adonis {vegan}) was conducted with 10,000 permutations. For both analyses, a Gower's dissimilarity matrix (daisy {cluster}) (Gower 1971) was calculated from z-score standardized morphological measures (scale {stats}). We tested for differences for each morphological measure between all supported clades in the phylogeny using analysis of variance (ANOVA, aov {stats}) or a Kruskal–Wallis rank sum test if they did not meet parametric assumptions (kruskal.test {stats}). All *P*-values were adjusted using a conservative Bonferroni correction (p.adjust {stats}) to minimize experiment-wide type I error. For characters that showed significant differences according to corrected *P*-values ($\alpha = 0.05$), we used Tukey's Honest Significant Difference (TukeyHSD {stats}) post hoc tests to determine pairwise differences among clades.

In order to identify which variables are important to discriminate between clades, a classification tree was conducted (CART, rpart {rpart}); the data did not meet the assumptions of a linear discriminant approach). For our CART model, the clade is the categorical response variable and the eight measures are the explanatory variables. Sixty randomly selected individuals with known genetic lineage

were chosen for the CART analysis, using the other 29 specimens to test the classification accuracy of the tree.

Type specimens of species that are currently synonymized with *E. fornicatus* were borrowed from the two largest scolytine collections: Natural History Museum Vienna (NHMW) and the National Museum of Natural History (NMNH) in Washington, DC. Holotypes or lectotypes of *E. fornicator*, *E. whitfordiodendrus*, *E. perbrevis*, *E. schultzei*, and *E. tapatapaoensis* were examined and measured to test if the specimens fit any of the clades defined here. We used our CART model to predict the clade membership of the synonymized type specimens.

Nomenclature

This paper and the nomenclatural act(s) it contains have been registered in Zoobank (www.zoobank.org), the official register of the International Commission on Zoological Nomenclature. The LSID (Life Science Identifier) number of the publication is: urn:lsid:zoobank.org:pub:C6345EBA-58D4-4790-925B-A07E55793614.

Results

Phylogenetic Reconstruction

The ML analysis confirmed three previously reported genetic lineages within the *E. fornicatus* species complex, and provided strong evidence for a fourth lineage (Fig. 2). From the individuals sequenced, and following the proposed nomenclature from Stouthamer et al. (2017), 36 corresponded to the PSHB clade, 10 corresponded to the KSHB, and 43 to the TSHB clade. Based on the phylogenetic tree and average pairwise distances, the TSHB clade was divided into two subclades, containing 36 individuals in the TSHBa (corresponds to clade 1B in Stouthamer et al. 2017) and seven in the TSHBb (corresponds to clade 1A in Stouthamer et al. 2017). Average K2P distances within and between each of the four clades are presented in Table 2. The status of *E. xanthopus* remains unclear: in our previous analysis (Stouthamer et al. 2017), *E. xanthopus* was resolved as closely related to the *E. fornicatus* complex, but our current analysis does not support a close relation of this species to TSHB.

Morphological Analysis

Of the 102 characters examined, only eight displayed variability that was diagnostic of at least one of the TSHBa, TSHBb, KSHB, and PSHB genetic lineages within the *E. fornicatus* complex: length of elytra, length of pronotum, width of elytra, width of pronotum, length-to-width ratio of pronotum and the elytra, length of the posterocoxal process, and number of socketed denticles in the protibia. The morphological analysis revealed significant variation among clades in the averages of these morphological characters, but there was also considerable degree of overlap (Fig. 3). All of the eight correlated characters were qualitative, none were discrete. The NMDS analysis represents the ordination of clades in two dimensions based on the morphological characters (Fig. 4). The PERMANOVA analysis showed that the four clades differ significantly in their morphology (pseudo-*F* = 18.45, *P*-value = 9.99 e-05).

Seven of the eight morphometric characters were significantly variable among the four clades of *Euwallacea*, the exception being the ratio of pronotum width to length (Table 3). Post hoc analysis revealed that KSHB and PSHB were significantly longer than TSHBa and TSHBb, and had significantly more elongated elytra (i.e., higher length-to-width ratio; Fig. 2). The number of protibial denticles was significantly higher for KSHB (median = 9) than PSHB (median = 8), though considerable overlap was observed. In general, TSHBa was larger and had more protibial denticles

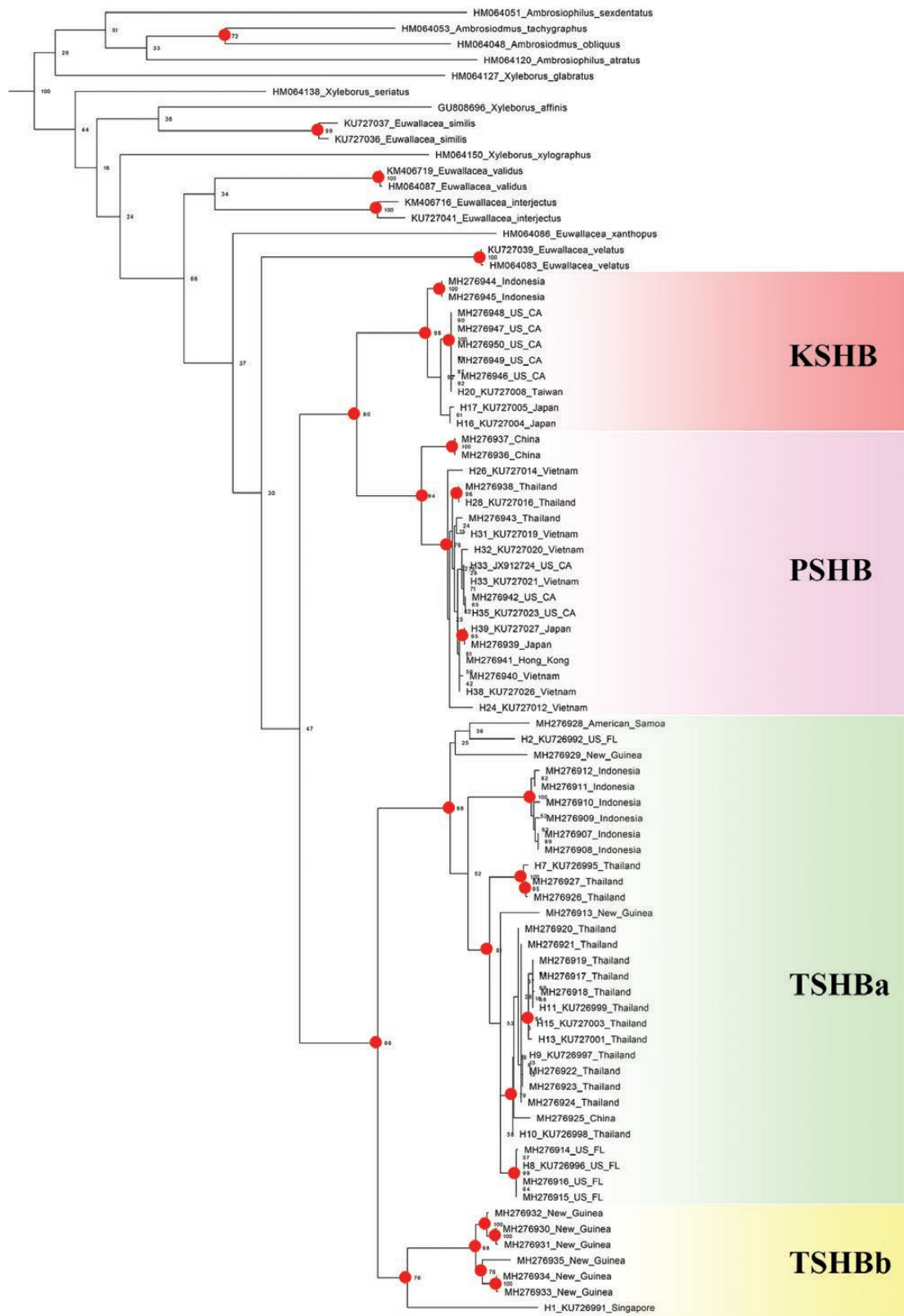


Fig. 2. ML phylogeny reconstruction of all measured individuals based on COI sequence. Red circles show bootstrap support over 70%.

than TSHBb. While these characters display significant mean differences between the four clades, the distributions of each partially overlap. No significant differences were found between well-supported subclades in the four main lineages (bootstrap > 70) TSHBa, TSHBb, PSHB, and KSHB.

The CART analysis classified the specimens into the four morphological categories that corresponded to phylogenetic clades (Fig. 5). The classification accuracy for the training data ($n = 60$) was 80%. The classification accuracy of the remaining individuals ($n = 29$) was 76%. The obtained classification tree indicates that the morphotype

Table 2. Average pairwise COI distance between representatives of phylogenetic clades within the *E. fornicatus* complex

Clade	TSHBa	TSHBb	PSHB	KSHB
TSHBa	0.057	0.129	0.144	0.140
TSHBb	0.144	0.059	0.145	0.148
PSHB	0.162	0.164	0.024	0.104
KSHB	0.156	0.167	0.114	0.018

Differences are calculated per site as p-distance (above diagonal) and Kimura two-parameter distance (K2P; below diagonal) using MEGA, version 6.06. Diagonal element shows within clade K2P.

identity was primarily explained by the elytra length and the pronotum length. The CART model also suggested that elytra ratio and pronotum width are important variables. The first node separated the PSHB and KSHB clades from the TSHB clade based on elytra length with 88% accuracy. Values lower than 1.55 mm in the elytra length correspond to the TSHB clade, where the second node separates the TSHBb from the TSHBa by a pronotum shorter than 1.05 mm with 83% accuracy. Within the PSHB-KSHB group, values lower than 1.74 mm for elytra length correspond to the PSHB clade with 78% accuracy.

The CART analysis classified the five type specimens into the pre-established clades. *Euwallacea fornicator* and *E. schultzei*

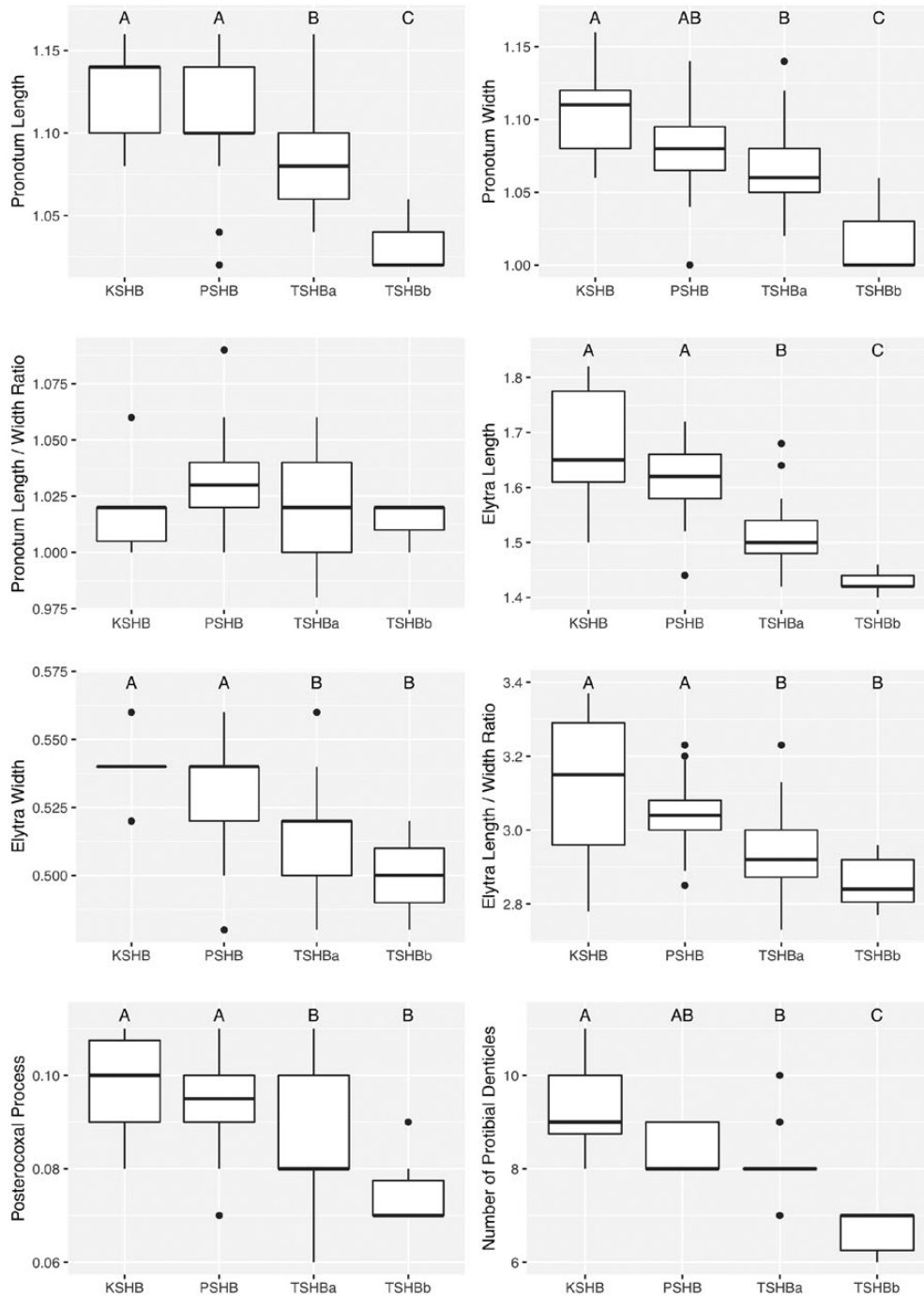


Fig. 3. Boxplots showing morphological characters variation among clades of *Euwallacea fornicatus* in the eight morphological characters that showed statistically significant correlation with at least one phylogenetic clade. Different letter above bars correspond to significant differences between clades (P -value < 0.05) in Tukey HSD (for ANOVA) and Dunn's test (for Kruskal–Wallis) comparisons.

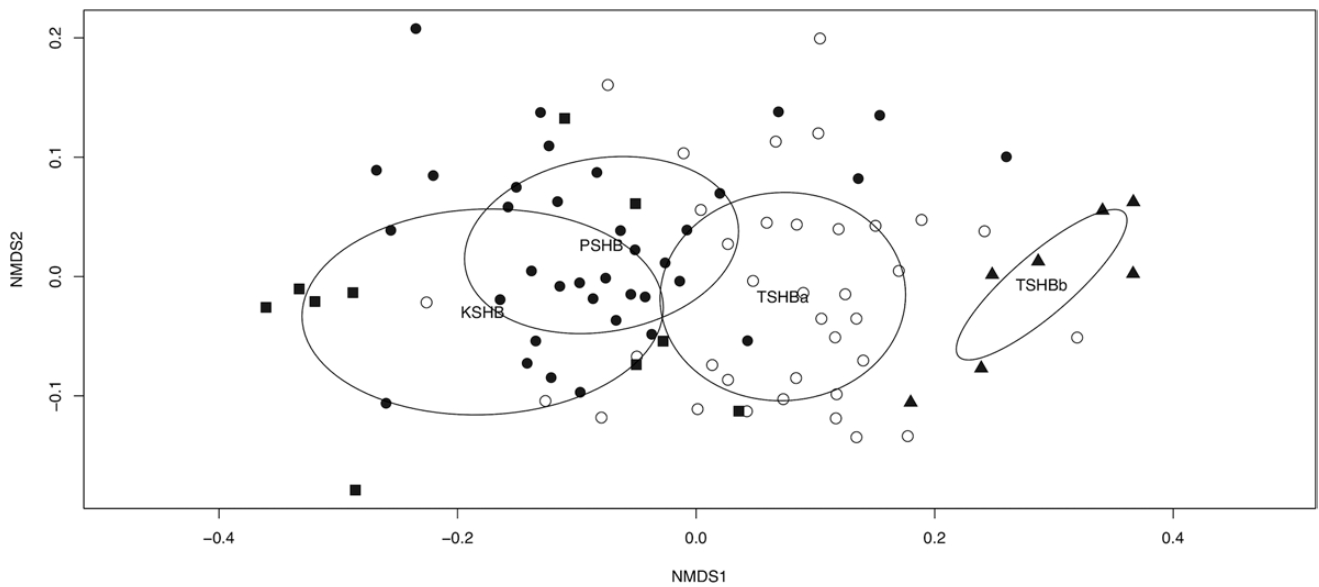


Fig. 4. Nonmetric multidimensional scaling plot of morphological distances of the eight morphological characters studied with ellipses showing one standard deviation around the centroid of each clade. Clade is indicated by shape: KSHB (square), PSHB (black circle), TSHBa (white circle), TSHBb (triangle). Stress = 0.138.

Table 3. Statistics and adjusted *P*-values from the ANOVA and Kruskal–Wallis analysis for the eight characters tested for morphological differences between the clades of *Euwallacea fornicatus*

Character	Test	Statistic	df	Adjusted <i>P</i> -value
Pronotum length	ANOVA	21.17	3, 85	<0.001
Elytra length	ANOVA	33.82	3, 85	<0.001
Pronotum width	ANOVA	12.85	3, 82	<0.001
Elytra width	ANOVA	12.60	3, 85	<0.001
Posterocoxal process length	ANOVA	8.98	3, 83	<0.001
Denticles	Kruskal–Wallis	28.95	3	<0.001
Pronotum ratio	ANOVA	3.68	3, 81	0.12
Elytra ratio	ANOVA	12.11	3, 85	<0.001

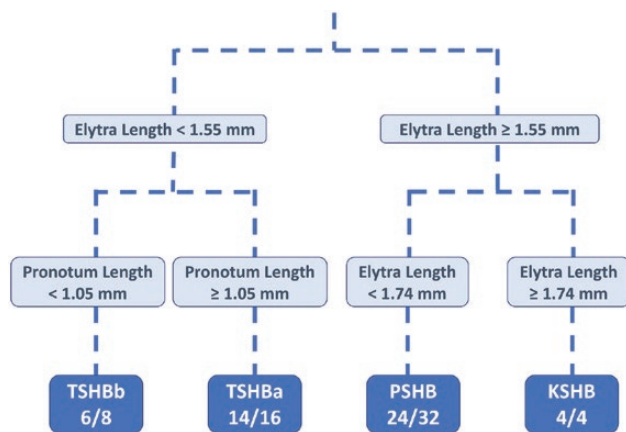


Fig. 5. Classification tree from the CART analysis built on 60 individuals representing the four clades within the *E. fornicatus* complex. Relevant characters for the node splits are shown. Classification rates are expressed as the number of correct classifications divided by the number of observations (individual beetles) in the node for the individuals used to train the CART model.

were classified into TSHBb. The lectotypes of *E. fornicator* and *E. schultzei* were collected in Sri Lanka and Philippines respectively. *Euwallacea whitfordiendrus* and *E. tapatapaensis* were classified

into PSHB, whereas *E. perbrevis* was classified into TSHBa. The lectotypes of *E. whitfordiendrus* and *E. tapatapaensis*, were collected in Malaysia and American Samoa, respectively, and the holotype of *E. perbrevis* was collected in the Philippines. None of the type specimens were assigned to the KSHB clade. As a result, we have proposed a new species name for this lineage. Based on the CART analysis, the location of the collected type material, and the distribution of the different clades, we suggest that individuals from the TSHBb should be referred to as *E. fornicator*, and individuals from the PSHB clade should be referred to as *E. whitfordiendrus*. Based on the collection information for the missing holotype of *E. fornicatus*, we suggest that individuals from the clade TSHBa should be referred to as *E. fornicatus* *Sensu stricto*.

Taxonomic Treatment

The following taxonomic changes are suggested considering the phylogenetic data, our CART analysis, and biogeographic concordance.

E. fornicatus Species Complex

Female: Length 1.8–2.9 mm; color dark brown to almost black. Frons broadly convex, surface mostly reticulate, punctures sparse. Antennal club type 3, posterior face of club with segments 2 and 3 partially visible (Hulcr et al. 2007). Pronotum as long as wide,



Fig. 6. Female *Euwallacea kuroshio* sp. nov. holotype, from top to bottom and left to right: lateral view, dorsal view, posterior oblique view of declivity, frontal view. Bar corresponds to 1.0 mm.

subcircular anteriorly, coarsely serrate; summit slightly behind middle; asperities in front of summit, smooth and reticulate behind. Elytra with striae and interstriae punctures in rows; striae not impressed, punctures moderately large, distinct, setae absent; interstriae three to four times as wide as striae, punctures uniseriate, rows of erect interstitial hairlike setae from base to apex. Declivity convex, gradually sloped; striae weakly impressed; interstitial denticles slightly larger than on disc. Posterolateral margin of declivity costate and broad. This species complex includes the four species from the classification tree revealed by the morphological analysis (Fig. 5). For final identification, DNA sequencing data will often be needed.

E. fornicatus (Eichhoff, 1868)

Xyleborus perbrevis Schedl, 1951: 59. Synonymy: Wood 1989.

Xyleborus schultzei Schedl, 1951: 68. Synonymy: Beaver 1991; Wood, 1989: 173.

Xyleborus tapatapaensis Schedl, 1951: 152. Synonymy: Wood 1989.

The syntypes of *E. fornicatus* from the Hamburg Museum collected in Sri Lanka were lost during World War II (Wood and Bright 1992). Based on the origin of the missing holotype, we refer to the TSHBa clade as *E. fornicatus* (Eichhoff 1868). Specimens within this clade have elytral length of 1.45–1.57 mm and a pronotum length of 1.05–1.11 mm, with 7 to 10 socketed denticles on the edge of

protibia. Pronotum width in this clade is 1.04–1.1 mm and elytra width is 0.5–0.54 mm. Distribution: Asia (American Samoa, China, Indonesia, Papua New Guinea, Samoa, Sri Lanka, Taiwan, Thailand), Australia, and introduced in United States (Florida and Hawaii).

Euwallacea fornicator (Eggers, 1923), stat. rev.

The lectotype of *E. fornicator* (NMNH) was classified as belonging to the TSHBb clade based on body measurements. The name *E. fornicator* (Eggers 1923), synonymized with *E. fornicatus* by Beeson (in 1930), is resurrected. Specimens within this clade are stouter than those of *E. fornicatus* s. str., with an elytra length of 1.41–1.45 mm and a pronotum length of 1.01–1.05 mm, with 6 or 7 socketed denticles on the margin of protibia. Pronotum width in this clade is 1–1.04 mm and elytra width is 0.48–0.52 mm. Distribution: Asia (Malaysia, Papua New Guinea, Singapore, Sri Lanka).

Euwallacea whitfordiodendrus (Schedl, 1942) stat. rev.

The lectotype of *E. whitfordiodendrus* (NHMW) was classified as belonging to the PSHB clade (the PSHB) based on body measures. The name *E. whitfordiodendrus* (Schedl 1942), synonymized with *E. fornicatus* by Wood (1989), is resurrected. Specimens within this clade have an elytra length of 1.55–1.67 mm and a pronotum length of 1.08–1.14 mm, with 8 or 9 socketed denticles on the margin of protibia. Pronotum width in this clade is 1.05–1.11 mm and elytra width is 0.51–0.55 mm. Distribution: Asia (China, Hong Kong, Japan, Taiwan, Thailand, and Vietnam) and introduced in United States (California), Israel, and Africa (South Africa).

Euwallacea kuroshio Gomez and Hulcr, sp. nov.

(Zoobank LSID: urn:lsid:zoobank.org:act:D8B5E6AD-D63B-4366-92FB-3EFA8C2BE80F)

The general morphology of the KSHB clade for particular body parts are as stated previously in the description of the *E. fornicatus* species complex. Specimens within this clade have an elytra length of 1.57–1.79 mm and a pronotum length of 1.09–1.15 mm, with 8 to 11 socketed denticles in the protibiae. Pronotum width in this species is 1.07–1.13 mm and elytra width is 0.53–0.55 mm.

Distribution

Asia (Indonesia, Japan, and Taiwan) and introduced in Mexico and United States (California).

Holotype Designation (Fig. 6)

Type Material: Holotype ♀: Japan, Okinawa, Naha, Shuri-Sueyoshi, February 2013. Hayato Masuya coll. (NMNH). Paratype ♀: Japan, Okinawa, Naha, Shuri-Sueyoshi, February 2013. Hayato Masuya coll. (Florida State Collection of Arthropods). Paratype ♀: Taiwan, Maolin District, Kaohsiung City, 2012. Naoto Kamata coll. (Florida State Collection of Arthropods).

Etymology

kuroshio is a noun in apposition and refers to the Kuroshio north-flowing ocean current between Taiwan and Okinawa known as the ‘Black Tide’, following Stouthamer et al. (2017). Holotype COI sequence: GenBank accession number KU727004.

Discussion

The phylogenetic analysis of COI for the *E. fornicatus* species complex identified four major clades corresponding largely, but not entirely, to distinct morphologies. Several subclades within each

major lineage were also supported by DNA sequence data, but no consistent morphological differences were found within the four major clades. Our results, therefore, corroborate the clades previously inferred by Stouthamer et al. (2017). In terms of geographical distribution, members of the four clades remain separated in their invaded ranges, but display significant overlap in native Asia and Oceania. The COI differences were large, ranging between 11 and 15% divergence between any of the four species. The difference in the sequences of *E. fornicatus* and *E. fornicatior* was also supported by our morphological analysis. This is notable because support for *E. fornicatus* and *E. fornicatior* was absent in the DNA sequences of two nuclear loci examined in the study of Stouthamer et al. (2017), suggesting that these are recently diverged species with no nuclear variation and a small number of morphological differences.

Few studies attempted to study an inbreeding scolytine species complex by combining morphological and molecular data. In the case of the globally invasive *Xylosandrus crassiusculus* (Motschulsky, 1866) (Curculionidae: Scolytinae), it was suggested that even morphologically and biologically homogeneous populations can display significant genomic polymorphism (Storer et al. 2017). In other cases of highly inbred scolytine beetles, however, detailed analysis of many populations revealed high COI divergence correlated with morphological differences, thus suggesting possible cryptic or incipient speciation (*Hypothenemus eruditus* (Westwood, 1836) (Curculionidae: Scolytinae), Kambestad et al. 2017). Our morphological validation of the *Euwallacea* clades corroborates recent suggestions of mating barriers, such as different clades preferring different pheromone ratios, and inter-clade mating resulting in lower fitness (Cooperband et al. 2017). The accumulated evidence therefore strongly supports the existence of multiple valid species.

The four clades differ morphologically on average, but even the most concordant measurements displayed notable overlap. This result challenges the typological species concept, and exemplifies the need for DNA-based barcoding for definitive species identification in cryptic complexes. Specimens from both *E. fornicatus* and *E. fornicatior* have shorter body length than *E. whitfordiodendrus* and *E. kuroshio*, primarily due to elytra length. Specimens of *E. fornicatior* differ from the rest of the species in the elytra and pronotum length-to-width ratios, showing stouter overall shape. Individuals of *E. whitfordiodendrus* present intermediate body lengths, whereas individuals of *E. kuroshio* present larger body sizes supported by the elytra length measures. Previous work by Chen et al. (2016) found significant differences between individuals from the TSHB and PSHB clades, the latter being significantly larger, based on measures of head width, pronotal width, body length, and ratio of body length to pronotal width. While independent measurements are not completely diagnostic in separating the species, they may be used to assign a probabilistic identification.

Knowledge of the *E. fornicatus* species complex has grown quickly in recent years, but identification of different members in published studies currently still relies on common names. Our morphological corroboration of this species complex now allows for the proper naming of the different genetic lineages based on museum material. Additionally, care has been taken to assign phylogenetic clades to type specimens not only based on morphology, but also on biogeographical provenance. Prior to this study, members of the *E. fornicatus* species complex could only be diagnosed with precision using DNA sequences of the COI gene. However, the morphological parameters inferred herein can be used by phytosanitary and border protection agencies in preliminary screening for potential new introductions outside the current range of the species. It is obvious, however, that morphology-based classification must be

considered tentative, and should be followed by DNA-based identification. Because of the overlap of morphological characters, DNA sequence typing provides a more robust and more reliable method for assessing species identity. Furthermore, the *E. fornicatus* species complex occurs over a vast area ranging from Oceania to Africa. New samples from this region often recover previously unknown diversity, including new phylogenetic clades. Therefore, each sample including ours should be considered a limited sub-sample of the entire diversity of haplotypes and morphologies. It seems likely that further sampling in this native range will reveal further phenotypic and genetic variation. Ideally, future analyses should include more specimens of the less abundant clades to define the size range with greater accuracy.

Conclusion

Our results suggest that the combination of an exhaustive character search and large-scale sampling, guided by some knowledge of genetic variation, can be a productive approach to resolving the taxonomy of cryptic species complexes. The resulting morphological species delimitation can be applied where a certain level of misclassification is permissible. This approach improves not only the fundamental understanding of organismal diversity, but also delivers practical, evidence-based guidance for species identification.

Supplementary Data

Supplementary data are available at *Insect Systematics and Diversity* online.

Acknowledgments

We thank Craig Bateman, Daniel Carrillo, Tom Coleman, Andrew J. Johnson, David Owens, Paul Kendra, You Li, Mark Schmaedick, and Caroline Storer for providing specimens. We also thank Lourdes Chamorro (USDA ARS) and Harald Shilhammer (Natural History Museum Vienna) for facilitating specimen loans. The authors also thank Sarah Smith, Bjarte Jordal, and the anonymous reviewers for their suggestions. The project was supported by the USDA Forest Service, the USDA-APHIS Farm Bill Section 10007, the Florida Department of Agriculture-Division of Plant Industry, the National Science Foundation, and a cooperative agreement with the USDA ARS.

References Cited

- Armstrong, K. F., and S. L. Ball. 2005. DNA barcodes for biosecurity: invasive species identification. *Phil. Trans. R. Soc.* 360: 1813–1823.
- Atkinson, T. H. 2017. Bark and Ambrosia Beetles. www.barkbeetles.info.
- Beaver, R. A. 1991. New synonymy and taxonomic changes in Pacific Scolytidae (Coleoptera). *Ann. des Naturhistorisches Museum Wien B.* 92: 87–97.
- Beeson, C. F. C. 1930. The biology of the genus *Xyleborus*, with more new species. *Ind. Forest Rec.* 14: 209–272.
- Boland, J. M. 2016. The impact of an invasive ambrosia beetle on the riparian habitats of the Tijuana River Valley, California. *PeerJ* 4: e2141.
- Brockerhoff, E. G., and A. M. Liebhold. 2017. Ecology of forest insect invasions. *Biol. Invasions.* 19: 1–19.
- Carrillo, D., L. Cruz, P. Kendra, T. Narvaez, W. Montgomery, A. Monterroso, A., C. De Grave, and M. Cooperband. 2016. Distribution, pest status and fungal associates of *Euwallacea* nr. *fornicatus* in Florida Avocado Groves. *Insects* 7: 55.
- Chen, Y., P. L. Dallara, L. J. Nelson, T. W. Coleman, S. M. Hishinuma, D. Carrillo, and S. J. Seybold. 2016. Comparative morphometric and chemical analyses of phenotypes of two invasive ambrosia beetles (*Euwallacea* spp.) in the United States of America. *Insect Sci.* 24: 647–662.

- Cooperband, M. F., A. A. Cossé, T. H. Jones, D. Carrillo, K. Cleary, I. Canlas and R. Stouthamer. 2017. Pheromones of three ambrosia beetles in the *Euwallacea fornicatus* species complex: ratios and preferences. PeerJ 5: e3957.
- Danthanarayana, W. 1968. The distribution and host-range of the shot-hole borer (*Xyleborus fornicatus* Eichh.) of tea. Tea Quarterly. 39: 61–69.
- Dodge, C., J. Carrillo, A. Eskalen, and R. Stouthamer. 2017. Evidence for symbiont promiscuity in two invasive ambrosia beetles (Coleoptera: Scolytinae: *Euwallacea* spp.), pp. 165. In Annual Meeting of the Entomological Society of America, 5 November 2017, Denver, CO.
- Eichhoff, W. 1868. Neue amerikanische Borkenkafer-Gattungen und Arten II. Berliner Entomologische Zeitschrift. 12: 145–152.
- Eskalen, A., A. Gonzalez, D. H. Wang, M. Twizeyimana, J. S. Mayorquin, and S. C. Lynch. 2012. First report of a *Fusarium* sp. and its vector tea shot hole borer (*Euwallacea fornicatus*) causing *Fusarium* dieback on avocado in California. Plant Dis. 96: 1070–1070.
- Folmer, O., M. Black, W. Hoeh, R. Lutz, and R. Vrijenhoek. 1994. DNA primers for amplification of mitochondrial cytochrome c oxidase subunit I from diverse metazoan invertebrates. Mol. March Biol. Biotechnol. 3: 294–299.
- Freeman, S., A. Protasov, M. Sharon, K. Mohotti, M. Elyahu, N. Okon-Levy, M. Maymon, and Z. Mendel. 2012. Obligate feed requirement of *Fusarium* sp. nov., an avocado wilting agent, by the ambrosia beetle *Euwallacea* aff. *fornicata*. Symbiosis. 58: 245–251.
- García-Avila, C. D. J., F. J. Trujillo-Arriaga, J. A. López-Buenfil, R. González-Gómez, D. Carrillo, L. F. Cruz, I. Ruiz-Galván, A. Quezada-Salinas, and N. Acevedo-Reyes. 2016. First report of *Euwallacea* nr. *fornicata* (Coleoptera: Curculionidae) in Mexico. Florida Entomol. 99: 555–556.
- Gower, J. C. 1971. A General Coefficient of Similarity and Some of Its Properties. Biometrics. 27: 857.
- Haack, R. 2001. Intercepted Scolytidae (Coleoptera) at US ports of entry: 1985–2000. Integr. Pest Manag. Rev. 6: 253–282.
- Haack, R. A., and R. J. Rabaglia. 2013. Exotic bark and ambrosia beetles in the USA: Potential and current invader, pp. 48–74. In J. E. Peña (ed.), Potential invasive pests of agricultural crops. CAB International, Boston, MA.
- Hulcr, J., S. A. Dole, R. A. Beaver, and A. I. Cognato. 2007. Cladistic review of generic taxonomic characters in Xyleborina (Coleoptera: Curculionidae: Scolytinae). Syst. Entomol. 32: 568–584.
- Hurley, B. P., B. Slippers, S. Sathyapala, and M. J. Wingfield. 2017. Challenges to planted forest health in developing economies. Biol. Invasions. 90: 1–13.
- Jordal, B., R. A. Beaver, and L. R. Kirkendall. 2001. Breaking taboos in the tropics: incest promotes colonization by wood-boring beetles. Glob. Ecol. Biogeogr. 10: 345–357.
- Kambestad, M., L. R. Kirkendall, I. L. Knutsen, and B. H. Jordal. 2017. Cryptic and pseudo-cryptic diversity in the world's most common bark beetle—*Hypothenemus eruditus*. Org. Divers. Evol. 17: 633–652.
- Kasson, M. T., K. O. Donnell, A. P. Rooney, S. Sink, R. C. Ploetz, J. N. Ploetz, J. L. Konkol, D. Carrillo, S. Freeman, Z. Mendel, et al. 2013. An inordinate fondness for *Fusarium*: phylogenetic diversity of fusaria cultivated by ambrosia beetles in the genus *Euwallacea* on avocado and other plant hosts. Fungal Genet. Biol. 56: 147–157.
- Katoh, K., and D. M. Standley. 2013. MAFFT multiple sequence alignment software version 7: improvements in performance and usability. Mol. Biol. Evol. 30: 772–780.
- Kearse, M., R. Moir, A. Wilson, S. Stones-Havas, M. Cheung, S. Sturrock, S. Buxton, A. Cooper, S. Markowitz, C. Duran, and T. Thierer. 2012. Geneious Basic: an integrated and extendable desktop software platform for the organization and analysis of sequence data. Bioinformatics. 28: 1647–1649.
- Kumar, S., G. Stecher, and K. Tamura. 2016. MEGA7: molecular evolutionary genetics analysis version 7.0 for bigger datasets. Mol. Biol. Evol. 33: 1870–1874.
- Li, Y., A. Lucky, and J. Hulcr. 2015. Tea Shot-Hole Borer *Euwallacea fornicatus* (Eichhoff, 1868) (Insecta: Coleoptera: Curculionidae: Scolytinae) IFAS Publication #EENY 624. University of Florida Institute of Food and Agricultural Sciences, Gainesville, FL. <https://edis.ifas.ufl.edu/in1090>.
- Mendel, Z., A. Protasov, M. Sharon, A. Zveibil, S. Ben Yehuda, K. O'Donnell, R. Rabaglia, M. Wysoki, and S. Freeman. 2012. An Asian ambrosia beetle *Euwallacea fornicatus* and its novel symbiotic fungus *Fusarium* sp. pose a serious threat to the Israeli avocado industry. Phytoparasitica 40: 235–238.
- Na, F., J. D. Carrillo, J. S. Mayorquin, C. Ndinga-Muniania, J. E. Stajich, R. Stouthamer, Y-T. Huang, Y-T. Lin, C-Y. Chen, and A. Eskalen. 2017. Two novel fungal symbionts *Fusarium kuroshium* sp. nov. and *Graphium kuroshium* sp. nov. of Kuroshio shot hole borer (*Euwallacea* sp. nr. *fornicata*) cause *Fusarium* dieback on woody host species in California. Plant Dis. 102: 1154–1164.
- O'Donnell, K., S. Sink, R. Libeskind-Hadas, J. Hulcr, M. T. Kasson, R. C. Ploetz, J. L. Konkol, J. N. Ploetz, D. Carrillo, A. Campbell, et al. 2015. Discordant phylogenies suggest repeated host shifts in the *Fusarium-Euwallacea* ambrosia beetle mutualism. Fungal Genet. Biol. 82: 277–290.
- Paap, T., W. de Beer, D. Migliorini, W. J. Nel, and M. J. Wingfield. 2018. The polyphagous shot hole borer (PSHB) and its fungal symbiont *Fusarium euwallaceae*: a new invasion in South Africa. Australas. Plant Pathol. 47: 1–7.
- Rabaglia, R. J., S. A. Dole, and A. I. Cognato. 2006. Review of American Xyleborina (Coleoptera: Curculionidae: Scolytinae) Occurring North of Mexico, with an Illustrated Key. Ann. Entomol. Soc. Am. 99: 1034–1056.
- R Development Core Team. 2017. R: A language and environment for statistical computing. R Foundation for Statistical Computing, Vienna, Austria. ISBN 3-900051-07-0, <http://www.R-project.org>.
- Stamatakis, A. 2014. RAxML version 8: a tool for phylogenetic analysis and post-analysis of large phylogenies. Bioinformatics. 30: 1312–1313.
- Storer, C., A. Payton, S. McDaniel, B. Jordal, and J. Hulcr. 2017. Cryptic genetic variation in an inbreeding and cosmopolitan pest, *Xylosandrus crassiusculus*, revealed using ddRADseq. Ecol. Evol. 1–13.
- Stouthamer, R., P. Rugman-Jones, P. Q. Thu, A. Eskalen, T. Thibault, J. Hulcr, L. J. Wang, B. H. Jordal, C. Y. Chen, M. Cooperband, et al. 2017. Tracing the origin of a cryptic invader: phylogeography of the *Euwallacea fornicatus* (Coleoptera: Curculionidae: Scolytinae) species complex. Agr. Forest Entomol. 19: 366–375.
- Susaeta, A., J. R. Soto, D. C. Adams, and J. Hulcr. 2016. Pre-invasion economic assessment of invasive species prevention: a putative ambrosia beetle in Southeastern loblolly pine forests. J. Environ. Manage. 183: 875–881.
- Wood, S. L. 1989. Nomenclatural changes and new species of Scolytidae (Coleoptera), Part IV. Great Basin Nat. 49: 167–185.
- Wood, S. L., and D. E. Bright. 1992. A catalog of Scolytidae and Platypodidae (Coleoptera), part 2: taxonomic index. Vols. A and B. Brigham Young University. Great Basin Naturalist Memoirs. 13: 1553.